IEEE Control Systems Letters paper presented at
2023 American Control Conference (ACC)
San Diego, CA, USA. May 31 - June 2, 2023

Robustness of two-dimensional stochastic dynamical wake models for yawed wind turbines

Mireille Rodrigues, Nicolas A. Burgess, Aditya H. Bhatt, Stefano Leonardi and Armin Zare

***Abstract*— We develop stochastic dynamical reduced-order models of wind farm turbulence that capture the effects of yaw misalignment due to control or atmospheric variability on turbine wakes and their interactions. Our models are based on the stochastically forced linearized Navier-Stokes equations around analytical descriptions of the wake velocity provided by low-fidelity engineering wake models. The power-spectral density of the source of additive stochastic excitation is identified via convex optimization to ensure statistical consistency with high-fidelity models while preserving model parsimony. We demonstrate the utility of our approach in capturing turbulence intensity variations in accordance with large-eddy simulations of the flow over a cascade of wind turbines. While our models are developed to match velocity correlations from sensors that are placed directly behind perfectly aligned wind turbine rotors, their predictions maintain a desirable level of accuracy even when the turbines are yawed.**

***Index Terms*— Control-oriented modeling, convex optimization, state covariances, stochastically forced Navier-Stokes equations, wake modeling, wind energy, yaw control.**

I. Introduction

Wake steering is one of the methods that have been proposed for reducing the power loss due to the operation of turbines in the wake of upwind ones [1]–[3]. Both numerical simulations and wind tunnel experiments have demonstrated the ability of yaw control in modulating the wake velocity and deflecting the wake away from downwind turbines [4]–[7]. While high-fidelity models, e.g., those that are based on the Reynolds-averaged Navier-Stokes (NS) or large-eddy simulations (LES), play an important role in improving our understanding of wake turbulence, due to their high computational cost, they are not suitable for developing real-time model-based control strategies that can adapt to time-varying atmospheric conditions.

Enabled by structural approximations such as the actuator disk model [8] and conservation principles for mass and momentum, low-fidelity engineering wake models have provided the means to bypass the need for high-fidelity models in wind farm planning and assessing the capabilities of turbine control strategies. Initial ventures in developing such models focused on two-dimensional (2D) heuristic-based methods that capture the steady-state hub-height velocity for prespecified atmospheric conditions [9]–[11]. More sophisticated variants that observed conservation principles [12], modeled the velocity deficit as a Gaussian distribution [13], or even incorporate 3D effects resulting from the ground or yawing [14], [15] were also combined with linear superposition laws to capture wake interactions over wind farms. Nevertheless, the over-simplified static nature of conventional engineering wake models that neglect the time-varying features of the near wake leads to the misrepresentation of wake recovery and inaccurate predictions of quantities of interest for wind farm control.

To overcome the shortcomings of static wake models, contributions have been made to add a degree of dynamics, e.g., the dynamic wake-meandering model [16], the dynamic extension of the Park model [17], or simplified variants of the NS equations [14], [18], [19]. In [20], [21], a stochastic dynamical wake modeling framework was proposed to augment the predictions of low-fidelity engineering wake models with a fluctuating velocity field whose dynamics are governed by the stochastically forced linearized NS equations. In this approach, the stochastic forcing is determined via convex optimization to ensure that the output of the linear model is consistent with LES in matching partially available power, thrust, or velocity intensity measurements across the farm.

Large and often rapid variations in the magnitude and direction of incoming wind can negatively impact the performance and structural durability of wind turbines. Thus, it is vital that forecasting models that are used to inform control algorithms account for atmospheric variations. Herein, we extend the work of Bhatt et al. [21] to develop stochastic dynamical models that account for second-order statistical signatures of the hub-height velocity field when turbine rotors are yawed away from the wind direction. The deflection of turbine wakes due to yaw misalignment is captured using a Gaussian wake model [22] around which the NS equations are linearized. While turbines are yawed away from the wind direction, we constrain the location of velocity correlations used in training the stochastic input to wind farm locations directly behind unyawed turbines. In spite of the constrained set of training data, our results support the robust performance our stochastic models in capturing wind variations that can be caused by atmospheric uncertainties.

The paper is organized as follows. In Sec. II, we formulate the problem and present our modeling approach. In Sec. III, we introduce the analytical base flow model for linearization. In Sec. IV, we linearize the NS equations around this profile and summarize the modeling framework used in shaping the forcing into the dynamics. In Sec. V, we train our models to match partially available velocity correlations at the hub-height of a cascade of 4 turbines and evaluate the robustness of our predictive models in the presence of yaw misalignment. We provide concluding remarks in Sec. VI.

M. Rodrigues, N. A. Burgess, A. H. Bhatt, S. Leonardi, and A. Zare are with the Department of Mechanical Engineering, University of Texas at Dallas, Richardson, TX 75080, USA. Corresponding author: armin.zare@utdallas.edu.

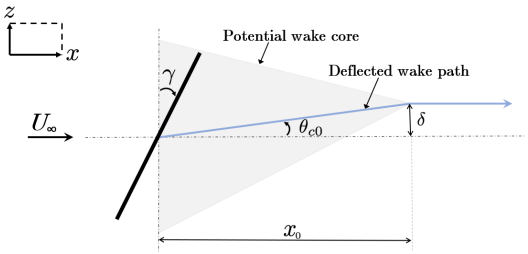

Fig. 1. The potential core (highlighted in grey) extends to a distance of x_0 beyond the hub. The wake centerline initially deflects at an angle θ_{c0} that depends on the rotor yaw angle γ (but counter-rotational to it). Beyond the core length, the wake centerline realigns the free-stream velocity.

II. Problem formulation

Engineering wake models provide analytical expressions for the velocity field that capture various structural aspects of spatially expanding wakes that are formed behind wind turbines. As such, the predictions of such static models may constitute a basic velocity profile around which fluctuations of the velocity field evolve. Based on this, the total wind velocity field $\mathbf{u}$ can be decomposed into the sum of the static base flow $\bar{\mathbf{u}}$ predicted by an engineering wake model and velocity fluctuations $\mathbf{v}$ that evolve around $\bar{\mathbf{u}}$, i.e.,

$$\mathbf{u} = \bar{\mathbf{u}} + \mathbf{v}. \tag{1}$$

Herein, we provide a reduced-order model for the dynamics of fluctuations $\mathbf{v}$ that augment the predictions of the low-fidelity analytical model $\bar{\mathbf{u}}$ by reproducing second-order statistics of wakes in accordance with high-fidelity simulations. More specifically, given a set of available velocity correlations at prespecified farm locations, the dynamics of $\mathbf{v}$ are sought to match the available statistics and complete the statistical signature of the turbulent flow.

We adopt a modeling framework that is based on stochastically forced linear time-invariant (LTI) approximations of complex dynamical systems represented by nonlinear partial differential equations (e.g., the NS equations) [23]–[25]. In this approach, the fluctuating component of the velocity field $\mathbf{v}$ is assumed to be a zero-mean Gaussian stochastic process whose evolution follows the state-space representation:

$$\begin{aligned} \boldsymbol{\psi}_t(\mathbf{x},t) &= A\,\boldsymbol{\psi}(\mathbf{x},t) + B\,\mathbf{d}(\mathbf{x},t) \\ \mathbf{v}(\mathbf{x},t) &= C\,\boldsymbol{\psi}(\mathbf{x},t). \end{aligned} \tag{2}$$

Here, $\boldsymbol{\psi}$ and $\boldsymbol{\psi}_t$ are the state and its partial derivative with respect to time t, $\mathbf{d}$ is a zero-mean stochastic process, A is the linear dynamic generator that approximates the nonlinear dynamics of the wake, B is the input operator that introduces the input $\mathbf{d}$ into the dynamics, and C is the output operator that establishes a kinematic relationship between $\boldsymbol{\psi}$ and $\mathbf{v}$.

In Sec. IV, we use the stochastically forced linearized NS equations as a physics-based model for the evolution of fluctuations $\mathbf{v}$ and determine $\mathbf{d}$ to match a partially available set of second-order velocity correlations. Leveraging the physics-based nature of the prior dynamical model represented by the linearized dynamic generator A, we demonstrate the robustness of Eqs. (2) in capturing the variance of the velocity field even when turbines are yawed from perfectly aligned (unyawed) training conditions. A finite-dimensional spatial approximation of the operators in Eq. (2) yields

$$\begin{aligned} \dot{\boldsymbol{\psi}}(t) &= A\,\boldsymbol{\psi}(t) + B\,\mathbf{d}(t) \\ \mathbf{v}(t) &= C\,\boldsymbol{\psi}(t) \end{aligned} \tag{3}$$

where $\boldsymbol{\psi}(t)$, $\mathbf{v}(t)$, $\mathbf{d}(t)$, A, B, and C are real-valued vectors and matrices of appropriate dimensions. We next provide details of an analytical wake model that accounts for the effects of yaw misalignment (e.g., wake deflection).

III. Base flow

We summarize the parameterization of a 3D Gaussian wake model proposed by Bastankhah and Porté-Agel [22], which accounts for the potential misalignment of the turbine rotor with respect to the wind direction. Figure 1 illustrates a wake zone predicted by a deficit-based wake model when the rotor axis is at an angle against the free-stream velocity U_∞ henceforth denoted as the yaw angle γ. The wake centerline deviates away from the wind direction at a deflection angle

$$\theta_{c0} = \frac{0.3\,\gamma}{\cos\gamma}\left(1 - \sqrt{1 - C_T\cos\gamma}\right)$$

where the thrust coefficient C_T is determined based on the properties of the turbine and its operating conditions for maximal power extraction. This deflection results in the spanwise shift δ of the streamwise velocity profile offered by the Gaussian wake model, i.e.,

$$\begin{aligned} U(x,z) = U_\infty - U_\infty &\left(1 - \sqrt{1 - \frac{C_T\cos\gamma}{8\,(\sigma_y\,\sigma_z/d_0^2)}}\right) \\ &\times \exp\left(-0.5\left[(\frac{y - y_h}{\sigma_y})^2 + (\frac{z-\delta}{\sigma_z})^2\right]\right) \end{aligned} \tag{4}$$

where d_0 is the non-dimensional rotor diameter, y_h is the hub height and the dependence of the wake width σ_z follows:

$$\begin{aligned} \frac{\sigma_y}{d_0} &= k\,\frac{x - x_0}{d_0} + \frac{1}{\sqrt{8}} \\ \frac{\sigma_z}{d_0} &= k\,\frac{x - x_0}{d_0} + \frac{\cos\gamma}{\sqrt{8}}. \end{aligned}$$

The spanwise wake deflection δ takes on different forms in near- and far-wake regions separated by a demarcation determined by the potential core length x_0 computed as

$$\frac{x_0}{d_0} = \frac{\cos\gamma\left(1 + \sqrt{1 - C_T}\right)}{\sqrt{2}\left(4\,\alpha\,I + \beta^\star\left(1 - \sqrt{1 - C_T}\right)\right)} \tag{5}$$

where α and $\beta^\star$ are constants, and I is the turbulence intensity, which is typically taken as a constant value. In the near-wake region ($x \le x_0$) $\delta := \theta_{c0}(x/d_0)$ and in the far-wake region ($x > x_0$),

$$\begin{aligned} \frac{\delta}{d_0} := \theta_{c0}\,\frac{x_0}{d_0} &+ \frac{\theta_{c0}}{14.7}\sqrt{\frac{\cos\gamma}{k\,C_T}}(2.9 + 1.3\sqrt{1 - C_T} - C_T) \\ &\times \ln\left[\frac{(1.6 + \sqrt{C_T})\left(1.6\sqrt{\frac{8\,\sigma_y\,\sigma_z}{d_0^2\cos\gamma}} - \sqrt{C_T}\right)}{(1.6 - \sqrt{C_T})\left(1.6\sqrt{\frac{8\,\sigma_y\,\sigma_z}{d_0^2\cos\gamma}} + \sqrt{C_T}\right)}\right] \end{aligned}$$

where k is the wake growth rate in the spanwise direction.

In a multi-turbine wind farm, the wake of upstream

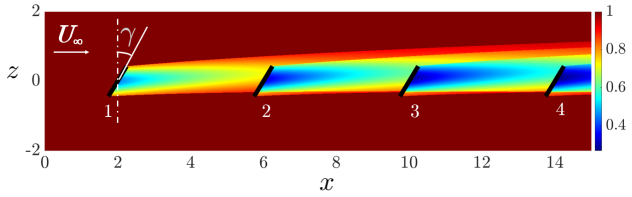

Fig. 2. Streamwise velocity predicted by Eq. (4) at the hub height of a wind farm with yawed turbines marked by thick black lines. The spatial domain is nondimensionalized by the rotor diameter (d_0).

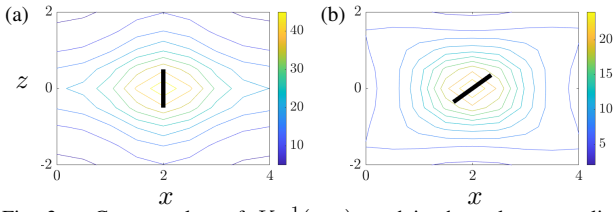

Fig. 3. Contour plots of $K^{-1}(x,z)$ used in the volume penalization technique for yaw angles (a) $\gamma = 0$ and (b) $\gamma = 45°$.

turbines affects the wake of downstream ones. Such interactions can be captured by linearly superposing the wakes of each turbine as predicted by Eq. (4). Figure 2 shows the streamwise velocity U predicted by this model for a cascade of 4 turbines that are uniformly yawed at an angle of 30°.

IV. Stochastic dynamical modeling

We assume knowledge of a structured set of second-order statistics of wind farm flow. This information, together with an initial prediction of the wind velocity $\bar{\mathbf{u}}$ from a low-fidelity engineering wake model such as the one presented in Sec. III can be used to complete the statistical signature of the flow in accordance with LTI system (3). In this section, we provide details on our particular choice of LTI model for the fluctuation field, namely the stochastically forced linearized NS equations, in addition to details on inverse problems that we formulate and solve to complete the statistical signature of the flow. While we linearize the NS equations around a profile extracted at the hub-height of the analytical model (4), the modeling approach is generalizable to 3D models.

A. Stochastically forced linearized Navier Stokes equation

The dynamics of small velocity and pressure fluctuations $(\mathbf{v}, p)$ around a base flow determined by $(\bar{\mathbf{u}}, \bar{P})$ are governed by the linearized NS and continuity equations

$$\begin{aligned} \mathbf{v}_t &= -(\nabla\cdot\mathbf{v})\,\bar{\mathbf{u}} - (\nabla\cdot\bar{\mathbf{u}})\,\mathbf{v} - \nabla p + \frac{1}{Re}\Delta\mathbf{v} - K^{-1}\mathbf{v} + \mathbf{d} \\ 0 &= \nabla\cdot\mathbf{v} \end{aligned} \tag{6}$$

where the base flow has a single non-zero component in the streamwise direction resulting from an engineering wake model (e.g., Eq. (4)), i.e., $\bar{\mathbf{u}} = [U \;\; 0]^T$, $\mathbf{v} = [u \;\; w]^T$ is the fluctuating velocity vector, with components u and w denoting velocity in the streamwise (x) and spanwise (z) directions, respectively, and $\mathbf{d}$ is a zero-mean stationary stochastic input that triggers a statistical response from the linear dynamics. Here, ∇ is the gradient operator, $\Delta = \nabla\cdot\nabla$ is the Laplacian, and the Reynolds number is defined in terms of the rotor diameter d_0, the free-stream velocity U_∞, and the kinematic viscosity ν as $Re = U_\infty d_0/\nu$. In these equations, length, velocity, time, and pressure have been nondimensionalized by d_0, U_∞, d_0/U_∞, and ρU_∞^2, respectively.

Equations (6) use a volume penalization technique to model the effect of solid obstructions to the flow caused by turbine structures. Instead of resolving the grid and and implementing no-slip/no-penetration boundary conditions over the surface of turbine structures, this method allows us to capture the effect of turbine rotors and nacelles (and even turbine towers in 3D models) by penalizing the velocity field using the negative feedback term $K^{-1}\mathbf{v}$. In this approach $K(x,z)$ plays the role of a 2D permeability function that only affects the velocity field at or around the coordinates of solid structures and has no influence on the flow at other spatial locations; see [26] for details. We note that the volume penalization function must be appropriately rotated to account for the orientation of the yawed turbine rotor. Figure 3 shows contour plots of sample K^{-1} functions.

A standard conversion for the elimination of pressure together with finite-dimensional approximation of the differential operators brings Eqs. (6) into the evolution form

$$\dot{\mathbf{v}}(t) \;=\; A\,\mathbf{v}(t) \;+\; B\,\mathbf{d}(t). \tag{7}$$

The form of system matrices A and B, along with details of the employed finite-dimensional approximation and boundary conditions on $\mathbf{v}$ can be found in [21, Appendix A]. The stochastic input $\mathbf{d}$ provides a degree of freedom for shaping the statistics of the velocity field $\mathbf{v}$. Under steady atmospheric conditions, system (7) is stable (A is Hurwitz). Thus, if (A, B) is a controllable pair, the steady-state covariance of the fluctuating velocity field $\mathbf{V} := \lim_{t\to\infty} \mathbf{E}\,[\mathbf{v}(t)\,\mathbf{v}^*(t)]$ resulting from persistent stochastic excitation of the linear dynamics solves the Lyapunov-like equation

$$A\,\mathbf{V} \;+\; \mathbf{V}A^* \;=\; -B\,H^* \;-\; H\,B^*. \tag{8}$$

This equation, which can be viewed as a generalization of the standard algebraic Lyapunov equation, relates the statistics of the state $\mathbf{v}$ to the spectral content of colored-in-time stochastic input $\mathbf{d}$. The entries of $\mathbf{V}$ represent two-point correlations of the velocity field at various spatial locations across the wind farm, with diagonal entries denoting one-point correlations or the intensity of the turbulent flow. Here, the matrix H quantifies the cross-correlation between the input and the state [24, Appendix B], i.e.,

$$H \;:=\; \lim_{t\to\infty} \mathbf{E}\,[\mathbf{v}(t)\,\mathbf{d}^*(t)] \;+\; \frac{1}{2}B\,\Omega.$$

See [23], [25] for additional details.

B. Identifying stochastic input via covariance completion

As we demonstrate in Sec. V, white-in-time stochastic input $\mathbf{d}$ is insufficient to account for the statistical signature of the turbulent wake behind turbines and better estimates of the turbulence intensity levels can be obtained via a stochastic realization informed by velocity statistics at prespecified wind farm locations. To this end, we adopt the stochastic dynamical modeling framework of Zare et

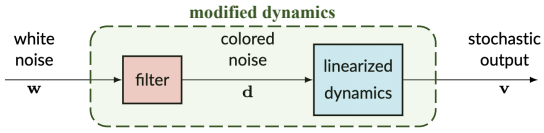

Fig. 4. A cascade connection of an LTI system with a linear filter that is designed to account for the sampled steady-state covariance matrix X.

al. [23]–[25], which has shown success in estimating the statistical signature of wind farm turbulence when turbine rotors are perpendicular to the wind direction [20], [21].

The velocity statistics that we use to train our stochastic models may be gathered via field experiments using, e.g., LiDAR measurement devices, or may result from high-fidelity LES simulations. As mentioned in the previous subsection, these one-point velocity correlations represent diagonal entries of covariance matrix $\mathbf{V}$. We seek input matrix B and statistics of forcing $\mathbf{d}$ that induce a statistical response from the linearized dynamics (7) that reproduces the partially known statistics. This information can be obtained from the solution to the covariance completion problem

$$\begin{aligned} \underset{\mathbf{V},Z}{\text{minimize}} \quad & -\log\det(\mathbf{V}) + \alpha\|Z\|_* \\ \text{subject to} \quad & A\mathbf{V} + \mathbf{V}A^* + Z = 0 \\ & \mathbf{V}_{i,j} = G_{i,j}, \quad \forall\,\{i,j\} \in \mathcal{I} \end{aligned} \tag{9}$$

which penalizes a composite objective subject to two linear constraints that (i) ensure statistical consistency with model (7) via the Lyapunov-like equation, and (ii) match partially known second-order statistics of the velocity field. In this convex optimization problem, Hermitian matrices $\mathbf{V}$ and Z are optimization variables, and entries of G corresponding to the set of indices $\mathcal{I}$ represent partially available second-order statistics of the output $\mathbf{v}$. The objective function establishes a trade-off (weighted by the parameter $\alpha > 0$) between the solution to a maximum-entropy problem, which uses the logarithmic barrier function to ensure positive definiteness of matrix $\mathbf{V}$, and a nuclear norm regularizer, which is used as a convex proxy for the rank function (see, e.g., [27], [28]). The rank of matrix Z bounds the number of independent input channels or columns in matrix B thereby providing a means to regulate the complexity of the forcing model as colored-in-time forcing $\mathbf{d}$ that excites all degrees of freedom can completely overwrite the linearized dynamics [23].

In addition to standard SDP solvers [29]–[31] that can be used to solve problem (9) for small-size systems, customized algorithms have been developed for larger systems [23], [32]. The solution to problem (9) can be used to realize the appropriate colored-in-time forcing $\mathbf{d}$ of system (7) such that the partially available velocity correlations are reproduced. Specifically, the matrix Z resulting from problem (9) can be decomposed into matrices B and H (cf. Eq. (8)) via spectral decomposition techniques. Matrix H can then be used to construct a low-pass filter that generates the suitable colored-in-time forcing $\mathbf{d}$ into the linearized dynamics (Fig. 4); see [23], [33] for additional details.

The parameterization of stochastic forcing relies on the solution to problem (9) and is thereby affected by the available training data (correlations of streamwise u and spanwise w velocity) indicated by set $\mathcal{I}$. As a result, atmospheric changes that may result in rapid variations in the intensity and direction of wind can jeopardize the validity of estimations provided by a stochastic model that is developed using a set of velocity correlations at prespecified wind farm locations. We next use a sequence of streamwise and spanwise velocity correlations from immediately behind turbine rotors to develop a stochastic model of wind farm turbulence and evaluate the robust performance of our modeling approach for different levels of yaw misalignment.

V. Numerical experiments

We provide a stochastic dynamical model for the hub-height turbulent velocity field of a cascade of 4 turbines that are uniformly yawed against the wind direction. In these experiments, $Re = 10^8$. We consider a computational domain of $L_x \times L_z = 15 \times 4$; $x \in [\,0,\ 15\,]$ and $z \in [\,-2,\ 2\,]$ with four turbines located at $x = \{2, 6, 10, 14\}$ and $z = 0$. We use $N_x = 22$ and $N_z = 9$ equally spaced collocation points to discretize the computational domain, which leads to a state of size $\mathbf{v} \in \mathbb{R}^{198\times 1}$ in model (7). The base flow for linearization of the NS equations is obtained using the analytical engineering wake model presented in Sec. III. For the results presented in this section, the diameter of turbines is set to $d_0 = 1$, the wake growth rate $k = 0.022$ is chosen in accordance with Ref. [22] for all yaw angles and the thrust coefficient $C_T = 0.7871$ corresponds to the maximum power generated by a 5MW NREL turbine [34] using an LES code that leverages blade momentum element theory [35], [36]. The turbulence intensity I is taken as 8% of the free-stream velocity in accordance with a precursor simulation that generates turbulent inflow conditions for LES. Following [22], the constant $\beta^\star = 0.154$ in Eq. (5) is determined under ideal conditions with no incoming turbulence ($I = 0$) to match the potential core length x_0 of jet flows. Moreover, given the turbulence intensity, $\alpha = 2$ is computed to best approximate the potential core length in accordance with the results of LES of flow behind a single turbine for various yaw angles.

Figure 5 highlights the necessity for colored-in-time forcing of the linear dynamics by comparing the streamwise turbulence intensity (uu) resulting from the linearized dynamics (7) subject to white-in-time forcing with the result of LES. The covariance of the white-in-time forcing has been adjusted using a scalar multiple of the identity ($\Omega = c_1\, I$) to match the maximum energy predicted by LES. It is evident that such white-in-time forcing cannot capture the dominant features of the yawed wake behind the wind turbines considered in this case study.

When the turbines are yawed, their wakes are deflected away from the wind direction thereby shifting the regions of highest turbulence intensity relative to reference non-yawed conditions. The base flow, and as a result, the linearized dynamics captured by the generator A in Eq. (7) adapt to the misalignment caused by the turbines' yaw. Nevertheless, in the pursuit of a practical training scheme that can adapt to the

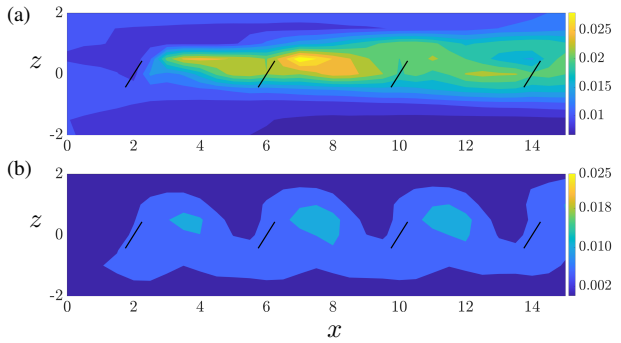

Fig. 5. Streamwise turbulence intensity at the hub height of a cascade of turbines yawed at $\gamma = 30^\circ$ predicted by (a) LES and (b) the linearized dynamics (7) subject to white-in-time stochastic forcing.

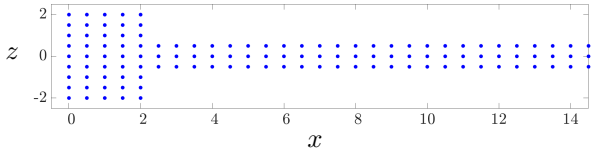

Fig. 6. Blue dots which represent the locations of training data using by optimization problem (9) cover the inflow region and all intermediate locations downstream of turbine nacelles and blade tips.

effects of wind variability and yaw control, we constrain the locations from which velocity correlations are collected to the inflow region upstream of the farm and the space immediately behind turbine rotors when facing the wind (Fig. 6). We provide access to LES-generated flow statistics (both uu and ww) within 3 diameters away from the turbines, which is in accordance with the quality of completion observed for the statistical signature of flow behind a single turbine [21].

Figure 7 compares the streamwise turbulence intensity uu predicted by our model and LES for cases with $\gamma = 15^\circ$ and 30°. While the energy of the flow is over-predicted by our model in certain parts of the farm, dominant features, including regions of high and low energy and the spanwise asymmetry of flow intensity due to the turbine's rotation, are particularly well captured. The high turbulence streams seen behind the blade tips at lower yaw coalesce into a single zone before dissipating upon incidence with the third turbine. Such features are also captured by our models. The good quality of predictions even for large yaw angles where a significant number of training data points do not fall within wake zone is attributed to the inherent physics-based nature of our models. Figure 8 provides a similar comparison for the spanwise turbulence intensity ww. The high spanwise intensity regions behind the turbine nacelles are generally well captured by our model albeit spurious regions of high intensity appear slightly beyond the blade tips and the wake zones. In contrast to the predictions of the streamwise turbulence intensity, we see that the quality of predictions improve as the yaw angle increases, which is especially evident for $\gamma = 30^\circ$.

VI. Concluding Remarks

We provide a stochastic modeling framework for augmenting the predictions of analytical engineering wake models by providing a fluctuating velocity field that captures the statistical signatures of wake turbulence in accordance with

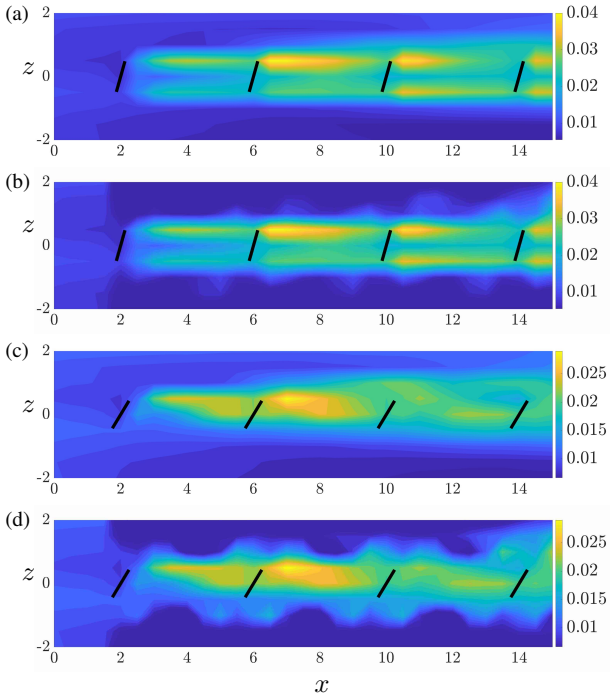

Fig. 7. The streamwise turbulence intensity uu at the hub height of a cascade of 4 turbines with uniform yaw angles of 15° (a,b) and 30° (c,d) resulting from LES (a,c) and our stochastic dynamical model (b,d).

high-fidelity simulations. Our models are based on the stochastically forced linearized NS equations around engineering wake models that account for the yaw misalignment of wind turbines due to control or atmospheric variability. The stochastic source of excitation to our linear models is determined via convex optimization to match a partially available set of velocity correlations at prespecified locations throughout the wind farm. In this paper, we have focused on the development of 2D models of hub-height turbulence. We demonstrate the robustness of our control-oriented model in predicting statistical signatures of the turbulent velocity field for different yaw angles even though the sensors that provide training data do not shift from non-yawed conditions (directly behind the turbine towers). Our ongoing efforts involve the development of 3D extensions of such a model that resolve the velocity field down to surfaces and enable ground sensing capabilities, the use of such models for sequential data-assimilation, e.g., Kalman filtering, and the adoption of alternative covariance completion formulations [33], [37] that can improve the quality of predictions.

Acknowledgments

This paper is based upon work partially supported by the National Science Foundation under grant numbers 1362022, 1362033, 1916715, and 1916776 (I/UCRC for Wind Energy, Science, Technology, and Research) and from the members of WindSTAR I/UCRC. Any opinions, findings, and conclusions or recommendations expressed in this material are those of the author(s) and do not necessarily reflect the views of the National Science Foundation or the sponsors. The Texas Advanced Computing Center is acknowledged for providing computing resources.

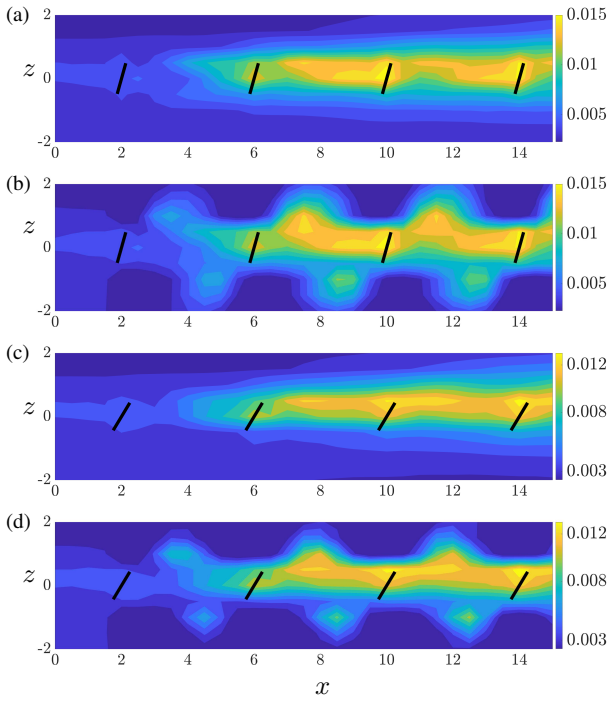

Fig. 8. The spanwise turbulence intensity ww at the hub height of a cascade of 4 turbines with uniform yaw angles of 15° (a,b) and 30° (c,d) resulting from LES (a,c) and our stochastic dynamical model (b,d).

REFERENCES

[1] P. Fleming, J. Annoni, J. J. Shah, L. Wan, S. Ananthan, Z. Zhang, K. Hutchings, P. Wang, W. Chen, and L. Chen, "Field test of wake steering at an offshore wind farm," *Wind Energy Sci.*, vol. 2, no. 1, pp. 229–239, 2017.

[2] M. F. Howland, K. S. Lele, and J. O. Dabiri, "Wind farm power optimization through wake steering," *Proc. Natl. Acad. Sci.*, vol. 116, no. 29, pp. 14 495–14 500, 2019.

[3] P. Fleming, J. King, E. Simley, J. Roadman, A. Scholbrock, P. Murphy, J. K. Lundquist, P. Moriarty, K. Fleming, J. van Dam, *et al.*, "Continued results from a field campaign of wake steering applied at a commercial wind farm–part 2," *Wind Energy Sci.*, vol. 5, no. 3, pp. 945–958, 2020.

[4] J. Å. Dahlberg and D. Medici, "Potential improvement of wind turbine array efficiency by active wake control (AWC)," in *Proceedings of the European Wind Energy Conference and Exhibition*, 2003, pp. 65–84.

[5] D. Medici and P. H. Alfredsson, "Measurements on a wind turbine wake: 3D effects and bluff body vortex shedding," *Wind Energy*, vol. 9, no. 3, pp. 219–236, 2006.

[6] Á. Jiménez, A. Crespo, and E. Migoya, "Application of a LES technique to characterize the wake deflection of a wind turbine in yaw," *Wind energy*, vol. 13, no. 6, pp. 559–572, 2010.

[7] P. A. Fleming, P. M. O. Gebraad, S. Lee, J.-W. van Wingerden, K. Johnson, M. Churchfield, J. Michalakes, P. Spalart, and P. Moriarty, "Evaluating techniques for redirecting turbine wakes using SOWFA," *Renew. Energy*, vol. 70, pp. 211–218, 2014.

[8] T. Burton, N. Jenkins, D. Sharpe, and E. Bossanyi, *Wind energy handbook*. John Wiley & Sons, 2011.

[9] N. O. Jensen, "A note on wind generator interaction," 1983.

[10] I. Katic, J. Højstrup, and N. O. Jensen, "A simple model for cluster efficiency," in *European wind energy association conference and exhibition*, vol. 1, 1986, pp. 407–410.

[11] J. F. Ainslie, "Calculating the flowfield in the wake of wind turbines," *J. Wind Eng. Ind. Aerodyn.*, vol. 27, no. 1-3, pp. 213–224, 1988.

[12] S. Frandsen, R. Barthelmie, S. Pryor, O. Rathmann, S. Larsen, J. Højstrup, and M. Thøgersen, "Analytical modelling of wind speed deficit in large offshore wind farms," *Wind Energy: An International Journal for Progress and Applications in Wind Power Conversion Technology*, vol. 9, no. 1-2, pp. 39–53, 2006.

[13] M. Bastankhah and F. Porté-Agel, "A new analytical model for wind-turbine wakes," *Renewable energy*, vol. 70, pp. 116–123, 2014.

[14] L. A. Martínez-Tossas, J. Annoni, P. A. Fleming, and M. J. Churchfield, "The aerodynamics of the curled wake: a simplified model in view of flow control," *Wind Energy Sci.*, vol. 4, no. 1, pp. 127–138, 2019.

[15] M. Bastankhah, C. R. Shapiro, S. Shamsoddin, D. F. Gayme, and C. Meneveau, "A vortex sheet based analytical model of the curled wake behind yawed wind turbines," *J. Fluid Mech.*, vol. 933, 2022.

[16] G. C. Larsen, H. A. Madsen, K. Thomsen, and T. J. Larsen, "Wake meandering: a pragmatic approach," *Wind Energy*, vol. 11, no. 4, pp. 377–395, 2008.

[17] J. Annoni, K. Howard, P. Seiler, and M. Guala, "An experimental investigation on the effect of individual turbine control on wind farm dynamics," *Wind Energy*, vol. 19, no. 8, pp. 1453–1467, 2016.

[18] M. Soleimanzadeh, R. Wisniewski, and A. Brand, "State-space representation of the wind flow model in wind farms," *Wind Energy*, vol. 17, no. 4, pp. 627–639, 2014.

[19] S. Boersma, M. Vali, M. Kühn, and J.-W. van Wingerden, "Quasi linear parameter varying modeling for wind farm control using the 2D Navier-Stokes equations," in *2016 American Control Conference (ACC)*. IEEE, 2016, pp. 4409–4414.

[20] A. H. Bhatt and A. Zare, "Toward stochastic dynamical wake-modeling for wind farms," in *Proceedings of the 2022 American Control Conference*, 2022, pp. 5241–5246.

[21] A. H. Bhatt, F. Bernardoni, S. Leonardi, and A. Zare, "Stochastic dynamical wake modeling for wind farms," *arXiv:2208.12196*, 2022.

[22] M. Bastankhah and F. Porté-Agel, "Experimental and theoretical study of wind turbine wakes in yawed conditions," *J. Fluid Mech.*, vol. 806, pp. 506–541, 2016.

[23] A. Zare, Y. Chen, M. R. Jovanovic, and T. T. Georgiou, "Low-complexity modeling of partially available second-order statistics: theory and an efficient matrix completion algorithm," *IEEE Trans. Automat. Control*, vol. 62, no. 3, pp. 1368–1383, March 2017.

[24] A. Zare, M. R. Jovanovic, and T. T. Georgiou, "Colour of turbulence," *J. Fluid Mech.*, vol. 812, pp. 636–680, February 2017.

[25] A. Zare, T. T. Georgiou, and M. R. Jovanovic, "Stochastic dynamical modeling of turbulent flows," *Annu. Rev. Control Robot. Auton. Syst.*, vol. 3, pp. 195–219, May 2020.

[26] K. Khadra, P. Angot, S. Parneix, and J. Caltagirone, "Fictitious domain approach for numerical modelling of Navier-Stokes equations," *Int. J. Numer. Methods Fluids*, vol. 34, no. 8, pp. 651–684, 2000.

[27] M. Fazel, "Matrix rank minimization with applications," Ph.D. dissertation, Stanford University, 2002.

[28] B. Recht, M. Fazel, and P. A. Parrilo, "Guaranteed minimum-rank solutions of linear matrix equations via nuclear norm minimization," *SIAM Rev.*, vol. 52, no. 3, pp. 471–501, 2010.

[29] K.-C. Toh, M. J. Todd, and R. H. Tütüncü, "SDPT3 — a MATLAB software package for semidefinite programming, version 1.3," *Optimization methods and software*, vol. 11, no. 1-4, pp. 545–581, 1999.

[30] M. Grant and S. Boyd, "CVX: Matlab Software for Disciplined Convex Programming, version 2.1," http://cvxr.com/cvx, Mar. 2014.

[31] S. Boyd and L. Vandenberghe, *Convex optimization*. Cambridge University Press, 2004.

[32] A. Zare, M. R. Jovanovic, and T. T. Georgiou, "Alternating direction optimization algorithms for covariance completion problems," in *Proceedings of the 2015 American Control Conference*, Chicago, IL, 2015, pp. 515–520.

[33] A. Zare, M. R. Jovanovic, and T. T. Georgiou, "Perturbation of system dynamics and the covariance completion problem," in *Proceedings of the 55th IEEE Conference on Decision and Control*, 2016, pp. 7036–7041.

[34] J. Jonkman, S. Butterfield, W. Musia, and G. Scott, "Definition of a 5-MW reference wind turbine for offshore system development," National Renewable Energy Lab. (NREL), Golden, CO, USA, Tech. Rep., 2009.

[35] C. Santoni, K. Carrasquillo, I. Arenas-Navarro, and S. Leonardi, "Effect of tower and nacelle on the flow past a wind turbine," *Wind Energy*, vol. 20, no. 12, pp. 1927–1939, 2017.

[36] C. Santoni, E. J. García-Cartagena, U. Ciri, L. Zhan, G. V. Iungo, and S. Leonardi, "One-way mesoscale-microscale coupling for simulating a wind farm in North Texas: Assessment against SCADA and LiDAR data," *Wind Energy*, vol. 23, no. 3, pp. 691–710, 2020.

[37] A. Zare, H. Mohammadi, N. K. Dhingra, T. T. Georgiou, and M. R. Jovanović, "Proximal algorithms for large-scale statistical modeling and sensor/actuator selection," *IEEE Trans. Automat. Control*, vol. 65, no. 8, pp. 3441–3456, August 2020.